J. Electroanal. Chem., 323 (1992) 1–27
Elsevier Sequoia S.A., Lausanne
JEC 01799

Multidimensional integral equations
Part 1. A new approach to solving microelectrode diffusion problems

Michael V. Mirkin and Allen J. Bard

Department of Chemistry, The University of Texas at Austin, Austin, TX 78712 (USA)

(Received 13 March 1991; in revised form 13 August 1991)

Abstract

The diffusion problems for a wide class of microelectrodes are shown to be reducible to multidimensional integral equations (equations containing multiple integrals). The formulation and solution of these problems by means of integral transformations are given for several types of microelectrode systems: a microdisk embedded in an insulating plane or in an insulator of a finite thickness, a microband, a scanning electrochemical microscope and an array of inlaid planar arbitrarily-shaped electrodes. Every solution obtained is suitable for a simple electrode reaction with any values of heterogeneous electron transfer kinetic parameters and for any shape of signal applied to the electrode. Analogous equations may be derived for some other mechanisms (e.g. electrochemical). The equations are similar to each other, and quite similar algorithms are required to solve them. No solutions of integral equations of this type have previously been published. An algorithm and FORTRAN programs for computing the polarization curves for the inlaid microdisk were devised, and chronoamperograms and cyclic voltammograms were computed. The derived equations and results are compared with known analytical solutions and simulations.

INTRODUCTION

The complexity of the mathematics used by electrochemists is always determined by the character of the objects they want to study. Up to the early 1950s, when the objects of electrochemical research were relatively simple (e.g. steady-state currents; uncomplicated electrode reactions at spherical liquid (mercury) electrodes or at planar electrodes), analytical solutions were available for most electrochemical systems considered [1]. Later, the incorporation of more complicated mechanisms and more complicated electrochemical methods led to the development of various types of semi-analytical techniques, such as integral equations [2–4] and infinite series [5]. These have largely been replaced by different variations of digital simulation [6,7], which appeared to be quite straightforward in the case of a complicated mechanism or special electrode geometry. Even these

powerful numerical (simulation) techniques have limitations, however. While they can be readily employed for processes with coupled chemical stages (especially of higher order), simulation of some systems with complex geometries (e.g. electrode arrays, partially blocked electrodes, rough electrodes) can require enormous computation times. Some systems can be simulated, but with some approximations. A well-known example involves electrochemistry at various planar microelectrodes [8]. For most of them, such as disk [9–24], band [25–27] or ring [28,29] electrodes, analytical and numerical solutions have been published which describe simple electrode processes or some mechanisms with coupled chemical reactions. However, the analytical (or semi-analytical) solutions are usually available only for simple situations, e.g. a current transient under diffusion control, and the numerical solutions do not meet all of the needs of the experimentalist; consequently, there is a large flow of new papers on the development of microelectrode theory (see, for example, refs 21–24, 29).

Previously [30,31], it was shown that by using integral equations one can uniformly describe a simple electrode reaction at planar or spherical electrodes, processes with coupled chemical reactions of the first order, or the nucleation–growth process under conditions of any electrochemical method. The algorithms [32,33] were always simpler than those in known numerical methods. We describe here a new semi-analytical technique which is quite general and can handle some problems that are difficult to simulate numerically.

THEORY

It is well known [34] that diffusion towards a uniformly accessible electrode (e.g. planar, spherical, or cylindrical) can be described by Fick's equation with one spatial variable. For a non-uniformly accessible electrode, the concentration distribution in general can be found from the three-dimensional Fick equation. Particular geometries which are important in practice usually possess some type of symmetry, allowing two-dimensional (2D) equations in rectangular (band) or cylindrical (disk, ring) coordinates to be used. We start with the 2D case.

Inlaid disk and rings

The diffusion problem for a simple electrode process in cylindrical coordinates is of the form:

$$\frac{\partial C_{Ox}}{\partial T} = D\left(\frac{\partial^2 C_{Ox}}{\partial Z^2} + \frac{\partial^2 C_{Ox}}{\partial R^2} + \frac{1}{R}\frac{\partial C_{Ox}}{\partial R}\right)$$

$$0 < Z,\ 0 \leq R,\ 0 < T \qquad (1)$$

$$\frac{\partial C_R}{\partial T} = D\left(\frac{\partial^2 C_R}{\partial Z^2} + \frac{\partial^2 C_R}{\partial R^2} + \frac{1}{R}\frac{\partial C_R}{\partial R}\right)$$

$$T=0,\ R\geq 0,\ Z>0 \qquad C_{Ox}(T,\ R,\ Z)=C^{\circ}_{Ox} \qquad C_R(T,\ R,\ Z)=0 \tag{2}$$

$$T>0,\ R+Z\to\infty \qquad C_{Ox}(T,\ R,\ Z)\to C^{\circ}_{Ox} \qquad C_R(T,\ R,\ Z)\to 0 \tag{3}$$

$$T>0,\ R\geq 0,\ Z=0$$

$$f_{Ox}(T,\ R)=D\left[\frac{\partial C_{Ox}(T,\ R,\ Z)}{\partial Z}\right]_{Z=0}=-D\left[\frac{\partial C_R(T,\ R,\ Z)}{\partial Z}\right]_{Z=0}=\frac{i(T,\ R)}{nF} \tag{4}$$

where

$$i(T,\ R)=nFk_s\{C_{Ox}(T,\ R)\exp\{-\alpha fn[E(T)-E^{\circ}]\} - C_R(T,\ R)\exp\{[1-\alpha]fn[E(T)-E^{\circ}]\}\} \tag{5}$$

and $f=F/RT$.

The total faradaic current is represented by

$$I(T)=2\pi\int_A i(T,\ R)R\ \mathrm{d}R \tag{6}$$

The above formulation contains two assumptions: (i) only one oxidized form is present in the solution initially, and (ii) diffusion coefficients of the oxidized and reduced forms are equal. The first assumption is chosen only because it was used in previous work. The second one leads to a well-known consequence

$$C_{Ox}(T,\ R,\ Z)+C_R(T,\ R,\ Z)=C^{\circ}_{Ox} \tag{7}$$

which allows one to solve for only C_{Ox} or C_R (eqn. (1)) and therefore makes the derivation much shorter. Actually, neither of these assumptions is essential for further consideration.

It should be noted that the boundary condition (4) holds for the conducting part of the electrode plane; for the insulating part, eqn. (4) holds with both the faradaic current and the diffusional flux equal to zero. Moreover, the conductive surface need not be continuous. Consequently, the given formulation is suitable not only for a disk or a ring, but also for any arrangement of a disk and a set of concentric rings (Fig. 1).

Using dimensionless variables

$$z=\frac{Z}{R_0} \qquad r=\frac{R}{R_0} \qquad t=\frac{DT}{R_0^2} \qquad c=1-\frac{C_{Ox}}{C^{\circ}_{Ox}}$$

$$f(t,\ r)=\left[\frac{\partial c(t,\ r,\ z)}{\partial z}\right]_{z=0}=-\frac{R_0}{C^{\circ}_{Ox}D}f_{Ox}(T,\ R) \tag{8}$$

and taking into account eqn. (7), one can rewrite the problem (eqns. (1)–(6)) as

$$\frac{\partial c}{\partial t}=\frac{\partial^2 c}{\partial z^2}+\frac{\partial^2 c}{\partial r^2}+\frac{1}{r}\frac{\partial c}{\partial r} \qquad 0<t,\ 0\leq r,\ 0<z \tag{9}$$

$$t=0,\ r\geq 0,\ z>0 \qquad c(t,\ r,\ z)=0 \tag{10}$$

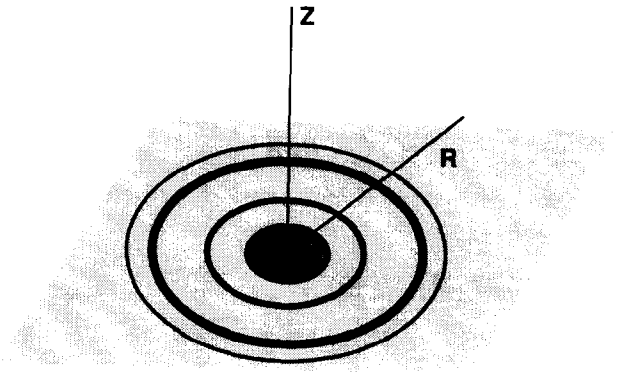

Fig. 1. A scheme of a planar system with cylindrical symmetry. The disk and surrounding rings are inlaid.

$$t > 0,\ r + z \to \infty \qquad c(t, r, z) \to 0 \tag{11}$$

$$t > 0,\ r \in \mathrm{A},\ \mathrm{z} = 0 \qquad f(t, r) = \frac{\left(1 + \exp\{fn[E(t) - E^{\circ}]\}\right)c(t, r) - 1}{\exp\{\alpha fn[E(t) - E^{\circ}]\}/\Lambda} \tag{12}$$

$$r \notin A \qquad f(t, r) = 0$$

$$I(t) = -2\pi \int_A f(t, r) r \, \mathrm{d}r \tag{13}$$

Applying a Hanckel transformation of order zero [35] with respect to r and a Laplace transformation with respect to t to eqns. (9) and (10) yields

$$s\bar{\bar{c}}(s, p, z) = \frac{\mathrm{d}^2\bar{\bar{c}}(s, p, z)}{\mathrm{d}z^2} - p^2\bar{\bar{c}}(s, p, z) \tag{14}$$

or

$$\frac{\mathrm{d}^2\bar{\bar{c}}(s, p, z)}{\mathrm{d}z^2} - (p^2 + s)\bar{\bar{c}}(s, p, z) = 0 \tag{15}$$

where $\bar{\bar{c}}(s, p, z)$ is the double transform of $c(t, r, z)$, s is a Laplace variable and p is a Hanckel variable. Solving this linear differential equation with the boundary condition of eqn. (11), we obtain (for $z = 0$)

$$\bar{\bar{c}}(s, p) = -\frac{\bar{\bar{f}}(s, p)}{(p^2 + s)^{1/2}} \tag{16}$$

where $\bar{\bar{c}}(s, p)$ and $\bar{\bar{f}}(s, p)$ are double transforms of $c(t, r)$ and $f(t, r)$ respectively.

Performing the inverse Laplace transformation (convolution) leads to

$$\bar{c}(t, p) = -\int_0^t \frac{\exp(-p^2(t-\tau))}{[\pi(t-\tau)]^{1/2}} \bar{f}(\tau, p)\, d\tau \tag{17}$$

Substituting the definition of the Hanckel transform [35]

$$\bar{f}(p) = \int_0^\infty u J_0(pu) f(u)\, du \tag{18}$$

where J_0 is a Bessel function of the first kind of order zero [36], into eqn. (17), we have

$$\bar{c}(t, p) = -\int_0^t \frac{\exp[-p^2(t-\tau)]}{[\pi(t-\tau)]^{1/2}}\, d\tau \int_0^\infty u J_0(pu) f(\tau, u)\, du \tag{19}$$

Now the inverse Hanckel transformation [35]

$$f(r) = \int_0^\infty p J_0(pr) \bar{f}(p)\, dp \tag{20}$$

yields

$$\begin{aligned} c(t, r) &= -\int_0^\infty p J_0(pr)\, dp \int_0^\infty u J_0(pu)\, du \int_0^t \frac{\exp[-p^2(t-\tau)]}{[\pi(t-\tau)]^{1/2}} f(\tau, u)\, d\tau \\ &= -\int_0^\infty u\, du \int_0^t \frac{f(\tau, u)}{[\pi(t-\tau)]^{1/2}}\, d\tau \int_0^\infty p \exp[-p^2(t-\tau)] J_0(pr) J_0(pu)\, dp \end{aligned} \tag{21}$$

According to Watson [37]

$$\int_0^\infty p \exp(-ap^2) J_0(rp) J_0(up)\, dp = \frac{1}{2a} \exp\left(-\frac{r^2+u^2}{4a}\right) I_0\left(\frac{ru}{2a}\right) \quad a > 0 \tag{22}$$

Thus we obtain

$$c(t, r) = -\frac{1}{2\sqrt{\pi}} \int_0^\infty u\, du \int_0^t \frac{\exp[-(r^2+u^2)/4(t-\tau)]}{(t-\tau)^{3/2}} I_0\left[\frac{ru}{2(t-\tau)}\right] f(\tau, u)\, d\tau \tag{23}$$

where I_0 is a modified Bessel function of the first kind of order zero [38]. The dummy variable of integration u is related to the radial distance. We introduce this notation to avoid confusion with r, which represents some fixed point.

Finally, the combination of eqns. (23) and (12) gives a two-dimensional second-kind integral equation:

$$\frac{f(t, r)\,\exp\{\alpha fn[E(t)-E^\circ]\}/\Lambda + 1}{1+\exp\{fn[E(t)-E^\circ]\}} = -\frac{1}{2\sqrt{\pi}}\int_0^\infty u\,du\int_0^t \frac{\exp[-(r^2+u^2)/4(t-\tau)]}{(t-\tau)^{3/2}} I_0\left[\frac{ru}{2(t-\tau)}\right] f(\tau, u)\,d\tau \quad (24)$$

It should be noted that the diffusional flux is equal to zero everywhere beyond the conductive surface A. Therefore the integration with respect to u in eqn. (24) should be performed over A, rather than from 0 to ∞. In the case of a disk electrode these limits are 0 and 1. Solving eqn. (24) with respect to $f(t, r)$, one can obtain a spatial distribution of the current on the electrode surface for any t, and the total dimensionless current is to be computed using eqn. (13). The dimensionless current is a function of two kinetic parameters Λ and αn.

Contemporary texts on integral equations [39,40] do not contain any information about solving multidimensional integral equations. Theoretical analysis and a few numerical examples can be found in the more advanced literature [41–43]. However, no algorithms for special cases are available. To our knowledge, no examples of the use of these equations in chemical, and particularly electrochemical, calculations have been reported. An approach to the numerical solution of multidimensional integral equations, as well as some computational results obtained from eqn. (24), will be discussed below.

Among several works containing analytical or semi-analytical solutions of the time-dependent microdisk problem, an approach developed by Fleischmann and coworkers [18–20] is closest to ours. In fact, if we did not perform an inverse Laplace transformation in eqn. (17), we would obtain, instead of eqn. (21), an expression for a Laplace transform of $\bar{c}(s, r)$ identical to eqn. (17) in ref. [19]. Fleischmann and coworkers derived their equation in a more complicated way using Neumann's integral theorem. These authors solved the integral equations in the Laplace domain and confronted the difficult problem of an approximate numerical inversion [20]. Also, they did not use eqn. (22) which allows one to get rid of a highly oscillating product of Bessel functions of the first kind. Consequently, the computer program given in ref. 20 is much more sophisticated than ours, and is suitable only for computing chronoamperograms of a diffusion-controlled process.

In refs 19 and 20 the derivation of the integral equations for the electrochemical (EC) mechanism under steady state conditions was shown to be essentially the same as the case of a simple electrode process. This is true for non-steady state conditions as well. Expressions similar to eqn. (24) can be derived for EC and perhaps for some other mechanisms with first-order chemical reactions.

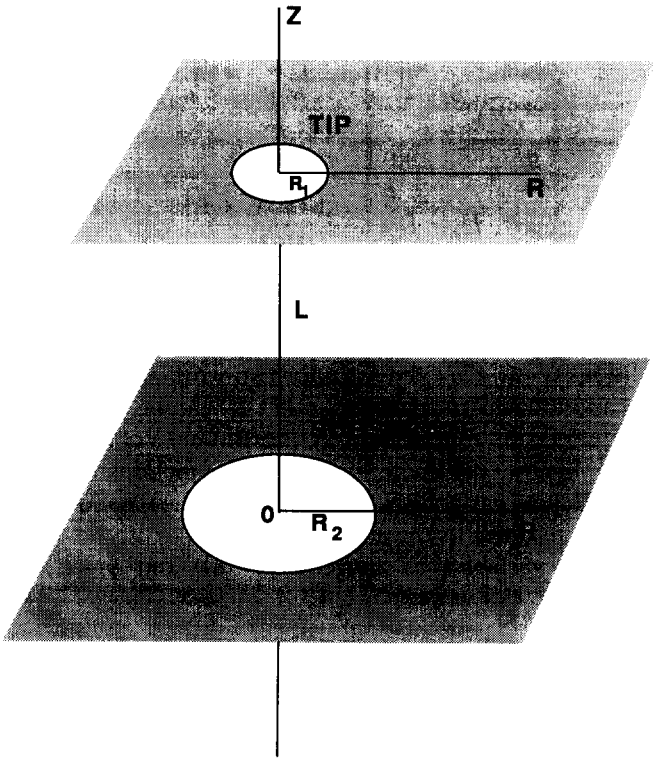

Fig. 2. A scheme of a scanning electrochemical microscope. A tip and a substrate are represented by arbitrarily-sized disk electrodes embedded in two parallel insulating planes. The centers of both electrodes are on the Z-axis.

Scanning electrochemical microscopy

The geometry in scanning electrochemical microscopy (SECM) [44] can be represented by two electrodes in close proximity (Fig. 2). One is a microdisk (tip); the other (substrate) may be of any size. The substrate can be taken as an infinitely large plane [45] or as having dimensions of the order of the tip.

In this case the diffusion problem

$$\frac{\partial C_{Ox}}{\partial T} = D\left(\frac{\partial^2 C_{Ox}}{\partial Z^2} + \frac{\partial^2 C_{Ox}}{\partial R^2} + \frac{1}{R}\frac{\partial C_{Ox}}{\partial R}\right)$$

$$0 < Z < L,\ 0 \leq R,\ 0 < T \tag{25}$$

$$\frac{\partial C_R}{\partial T} = D\left(\frac{\partial^2 C_R}{\partial Z^2} + \frac{\partial^2 C_R}{\partial R^2} + \frac{1}{R}\frac{\partial C_R}{\partial R}\right)$$

$$T = 0,\ R \geq 0,\ L > Z > 0 \qquad C_{Ox}(T, R, Z) = C^{\circ}_{Ox} \qquad C_R(T, R, Z) = 0 \tag{26}$$

$$T>0,\ R_1>R\geq 0,\ Z=0 \qquad f_{Ox}(T,\ R,\ 0)=D\left[\frac{\partial C_{Ox}(T,\ R,\ Z)}{\partial Z}\right]_{Z=0}$$

$$=-D\left[\frac{\partial C_R(T,\ R,\ Z)}{\partial Z}\right]_{Z=0}=\frac{i_1(T,\ R)}{nF} \tag{27}$$

$$T>0,\ R_2>R\geq 0,\ Z=L \qquad f_{Ox}(T,\ R,\ L)=D\left[\frac{\partial C_{Ox}(T,\ R,\ Z)}{\partial Z}\right]_{Z=L}$$

$$=-D\left[\frac{\partial C_R(T,\ R,\ Z)}{\partial Z}\right]_{Z=L}=-\frac{i_2(T,\ R)}{nF} \tag{28}$$

includes two boundary conditions (eqns. (27) and (28)) for two working electrodes. Both the tip current $i_1(T,\ R)$ and the substrate current $i_2(T,\ R)$ can be affected by electron transfer (ET) kinetic effects as represented by the Butler–Volmer equation (eqn. (5)). However, the kinetic parameters and $E(t)$ functions may be different at the two electrodes. Below, variables with subscript 1 correspond to the tip and those with subscript 2 correspond to the substrate.

Using the same dimensionless variables as above (eqn. (8)) and $\gamma=L/R_1$, $\delta=R_2/R_1$, and recalling eqn. (6) we can write

$$\frac{\partial c}{\partial t}=\frac{\partial^2 c}{\partial z^2}+\frac{\partial^2 c}{\partial r^2}+\frac{1}{r}\frac{\partial c}{\partial r} \qquad 0<t,\ 0\leq r,\ 0<z<\gamma \tag{29}$$

$$t=0,\ 0\leq r,\ 0<z<\gamma \qquad c(0,\ r,\ z)=0 \tag{30}$$

$$0<t,\ 0\leq r<1,\ z=0 \qquad f_1(t,\ r)=\frac{\left[1+\exp\{fn[E_1(t)-E^\circ]\}\right]c_1(t,\ r)-1}{\exp\{\alpha_1 fn[E_1(t)-E^\circ]\}/\Lambda_1}$$

$$1<r,\ f_1(t,\ r)=0 \tag{31}$$

$$0<t,\ 0\leq r<\delta,\ z=\gamma \qquad f_2(t,\ r)=-\frac{\left[1+\exp\{fn[E_2(t)-E^\circ]\}\right]c_2(t,\ r)-1}{\exp\{\alpha_2 fn[E_2(t)-E^\circ]\}/\Lambda_2}$$

$$\delta<r,\ f_2(t,\ r)=0 \tag{32}$$

$$I_1(t)=-2\pi\int_0^1 f_1(t,\ r)r\ \mathrm{d}r \qquad I_2(t)=2\pi\int_0^\delta f_2(t,\ r)r\ \mathrm{d}r \tag{33}$$

Applying Laplace and Hanckel transformations to eqns. (29) and (30), as was done above, we again obtain eqn. (15):

$$\frac{\mathrm{d}^2\bar{\bar{c}}(s,\ p,\ z)}{\mathrm{d}z^2}-(p^2+s)\bar{\bar{c}}(s,\ p,\ z)=0$$

with two boundary conditions:

$$z=0 \qquad \frac{\mathrm{d}\bar{\bar{c}}(s,\ p,\ z)}{\mathrm{d}z}=\overline{\bar{f}}_1(s,\ p) \tag{34}$$

$$z=\gamma \qquad \frac{\mathrm{d}\bar{\bar{c}}(s,\ p,\ z)}{\mathrm{d}z}=\overline{\bar{f}}_2(s,\ p) \tag{35}$$

The solution of this boundary value problem is

$$\overline{\overline{c_1}}(s, p) = \frac{\overline{\overline{f_2}}(s, p) - \overline{\overline{f_1}}(s, p) \cosh\left[\gamma(p^2+s)^{1/2}\right]}{(p^2+s)^{1/2} \sinh\left[\gamma(p^2+s)^{1/2}\right]} \tag{36}$$

$$\overline{\overline{c_2}}(s, p) = \frac{\overline{\overline{f_2}}(s, p) \cosh\left[\gamma(p^2+s)^{1/2}\right] - \overline{\overline{f_1}}(s, p)}{(p^2+s)^{1/2} \sinh\left[\gamma(p^2+s)^{1/2}\right]} \tag{37}$$

In this case inverse Laplace transformation yields [46]

$$\overline{c_1}(t, p) = \frac{1}{\gamma}\int_0^t \exp\left[-p^2(t-\tau)\right] \times \left\{\overline{f_2}(\tau, p)\theta_4\left[0\middle|\frac{i\pi(t-\tau)}{\gamma^2}\right] - \overline{f_1}(\tau, p)\theta_3\left[0\middle|\frac{i\pi(t-\tau)}{\gamma^2}\right]\right\} d\tau \tag{38}$$

$$\overline{c_2}(t, p) = \frac{1}{\gamma}\int_0^t \exp\left[-p^2(t-\tau)\right] \times \left\{\overline{f_2}(\tau, p)\theta_3\left[0\middle|\frac{i\pi(t-\tau)}{\gamma^2}\right] - \overline{f_1}(\tau, p)\theta_4\left[0\middle|\frac{i\pi(t-\tau)}{\gamma^2}\right]\right\} d\tau \tag{39}$$

where θ_3 and θ_4 are theta functions [47]. Using the definitions of the Hanckel transform and the inverse Hanckel transform of order zero (eqns. (18) and (20)), we obtain

$$c_1(t, r) = \frac{1}{\gamma}\int_0^\infty pJ_0(pr)\, dp \int_0^\infty uJ_0(pu)\, du \times \int_0^t \exp\left[-p^2(t-\tau)\right] \times \left\{f_2(\tau, u)\theta_4\left[0\middle|\frac{i\pi(t-\tau)}{\gamma^2}\right] - f_1(\tau, u)\theta_3\left[0\middle|\frac{i\pi(t-\tau)}{\gamma^2}\right]\right\} d\tau \tag{40}$$

$$c_2(t, r) = \frac{1}{\gamma}\int_0^\infty pJ_0(pr)\, dp \int_0^\infty uJ_0(pu)\, du \times \int_0^t \exp\left[-p^2(t-\tau)\right] \times \left\{f_2(\tau, u)\theta_3\left[0\middle|\frac{i\pi(t-\tau)}{\gamma^2}\right] - f_1(\tau, u)\theta_4\left[0\middle|\frac{i\pi(t-\tau)}{\gamma^2}\right]\right\} d\tau \tag{41}$$

Using eqn. (22) gives

$$c_1(t, r) = \frac{1}{2\gamma}\int_0^\infty u\,\mathrm{d}u \int_0^t \frac{\exp\left[-(r^2+u^2)/4(t-\tau)\right]}{t-\tau} \times I_0\left[\frac{ru}{2(t-\tau)}\right] \times \left\{ f_2(\tau, u)\theta_4\left[0\middle|\frac{i\pi(t-\tau)}{\gamma^2}\right] - f_1(\tau, u)\theta_3\left[0\middle|\frac{i\pi(t-\tau)}{\gamma^2}\right]\right\} \mathrm{d}\tau \qquad (42)$$

$$c_2(t, r) = \frac{1}{2\gamma}\int_0^\infty u\,\mathrm{d}u \int_0^t \frac{\exp\left[-(r^2+u^2)/4(t-\tau)\right]}{t-\tau} \times I_0\left[\frac{ru}{2(t-\tau)}\right] \times \left\{ f_2(\tau, u)\theta_3\left[0\middle|\frac{i\pi(t-\tau)}{\gamma^2}\right] - f_1(\tau, u)\theta_4\left[0\middle|\frac{i\pi(t-\tau)}{\gamma^2}\right]\right\} \mathrm{d}\tau \qquad (43)$$

Combining eqns. (42), (43), (31) and (32) results in

$$\frac{f_1(t, r)\,\exp(\alpha_1 fn[E_1(t) - E^\circ])/\Lambda_1 + 1}{1 + \exp\{fn[E_1(t) - E^\circ]\}} = \frac{1}{2\gamma}\int_0^\infty u\,\mathrm{d}u \int_0^t \frac{\exp\left[-(r^2+u^2)/4(t-\tau)\right]}{t-\tau} \times I_0\left[\frac{ru}{2(t-\tau)}\right]\left\{ f_2(\tau, u)\theta_4\left[0\middle|\frac{i\pi(t-\tau)}{\gamma^2}\right] - f_1(\tau, u)\theta_3\left[0\middle|\frac{i\pi(t-\tau)}{\gamma^2}\right]\right\} \mathrm{d}\tau \qquad (44)$$

$$\frac{1 - f_2(t, r)\,\exp(\alpha_2 fn[E_2(t) - E^\circ])/\Lambda_2}{1 + \exp\{fn[E_2(t) - E^\circ]\}} = \frac{1}{2\gamma}\int_0^\infty u\,\mathrm{d}u \int_0^t \frac{\exp\left[-(r^2+u^2)/4(t-\tau)\right]}{t-\tau} \times I_0\left[\frac{ru}{2(t-\tau)}\right]\left\{ f_2(\tau, u)\theta_3\left[0\middle|\frac{i\pi(t-\tau)}{\gamma^2}\right] - f_1(\tau, u)\theta_4\left[0\middle|\frac{i\pi(t-\tau)}{\gamma^2}\right]\right\} \mathrm{d}\tau \qquad (45)$$

which are the desired solutions for SECM. Equations (44) and (45), like eqn. (24), are suitable for any values the kinetic parameters and for any functions $E_1(t)$ and $E_2(t)$. When the substrate is insulating, $f_2(t, r) = 0$, and only eqn. (44) needs to be

solved, resulting in a simpler problem. These equations look somewhat more complicated than those derived for a microdisk; however, the numerical algorithm to solve these, which is currently under development, is essentially the same. Taking into account that

$$\theta_3\left(0\middle|\frac{i\pi t}{\gamma^2}\right) = \frac{\gamma}{(\pi t)^{1/2}}\left[1 + 2\sum_{n=1}^{\infty}\exp\left(-\frac{n^2\gamma^2}{t}\right)\right]$$

and

$$\theta_4\left(0\middle|\frac{i\pi t}{\gamma^2}\right) = \frac{2\gamma}{(\pi t)^{1/2}}\sum_{n=1}^{\infty}\exp\left[-\frac{(n-0.5)^2\gamma^2}{t}\right]$$

one can see that as $\gamma \to \infty$, eqns. (44) and (45) describe two independent microdisks (eqn. (24)).

It should be noted that eqns. (44) and (45) rely on the assumption that both the tip and the substrate are embedded in insulating planes. This is not completely consistent with real SECM conditions. A way to avoid this limitation is shown later.

Microband electrode

Unlike the two previous cases, the two-dimensional diffusion problem for the microband requires rectangular coordinates:

$$\frac{\partial C_{Ox}}{\partial T} = D\left(\frac{\partial^2 C_{Ox}}{\partial X^2} + \frac{\partial^2 C_{Ox}}{\partial Z^2}\right)$$

$$0 < T,\ -\infty < X < \infty,\ 0 < Z \tag{46}$$

$$\frac{\partial C_R}{\partial T} = D\left(\frac{\partial^2 C_R}{\partial X^2} + \frac{\partial^2 C_R}{\partial Z^2}\right)$$

$$T = 0,\ -\infty < X < \infty,\ 0 < Z \qquad C_{Ox}(T, X, Z) = C^\circ_{Ox} \qquad C_R(T, X, Z) = 0 \tag{47}$$

$$0 < T,\ X^2 + Z \to \infty \qquad C_{Ox}(T, X, Z) \to C^\circ_{Ox} \qquad C_R(T, X, Z) \to 0 \tag{48}$$

$$0 < T,\ -\infty < X < \infty,\ Z = 0$$

$$f_{Ox}(T, X) = D\left[\frac{\partial C_{Ox}(T, X, Z)}{\partial Z}\right]_{Z=0} = -D\left[\frac{\partial C_R(T, X, Z)}{\partial Z}\right]_{Z=0} = \frac{i(T, X)}{nF} \tag{49}$$

The dimensionless variables in this case are

$$x = \frac{2X}{w},\ z = \frac{2Z}{w},\ t = \frac{4DT}{w^2},\ c = 1 - \frac{C_{Ox}}{C^\circ_{Ox}}$$

$$f(t, x) = \left[\frac{\partial c(t, x, z)}{\partial z}\right]_{z=0} = -\frac{w}{2DC^\circ_{Ox}} f_{Ox}(T, X) \tag{50}$$

and the dimensionless form of the problem is

$$\frac{\partial c}{\partial t} = \frac{\partial^2 c}{\partial z^2} + \frac{\partial^2 c}{\partial x^2} \qquad 0 < t,\ -\infty < x < \infty,\ 0 < z \tag{51}$$

$$t = 0,\ -\infty < x < \infty,\ 0 < z \qquad c(t, x, z) = 0 \tag{52}$$

$$0 < t,\ x^2 + z \to \infty \qquad c(t, x, z) \to 0 \tag{53}$$

$$0 < t,\ x \in A,\ z = 0 \qquad f(t, x) = \frac{(1 + \exp\{fn[E(t) - E^\circ]\})c(t, x) - 1}{\exp\{\alpha fn[E(t) - E^\circ]\}/\Lambda}$$

$$x \notin A,\ f(t, x) = 0 \tag{54}$$

$$I(t) = -\int_A f(t, x)\, \mathrm{d}x \tag{55}$$

Applying a Fourier transformation with respect to x and a Laplace transformation with respect to t, as was done in ref. 25 for example, we come to a differential

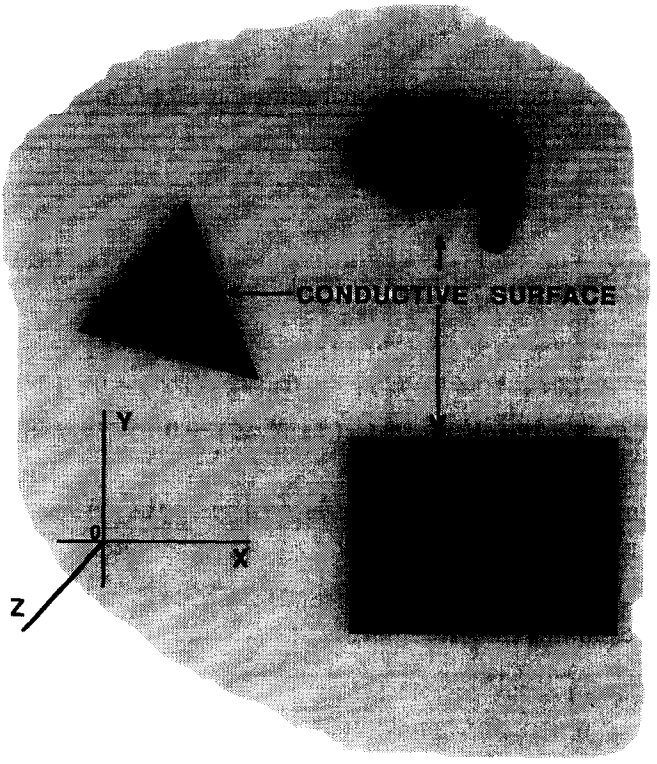

Fig. 3. An assembly of inlaid planar electrodes of an arbitrary shape. The X and Y axes refer to the electrode plane.

equation formally identical with eqn. (15):

$$\frac{d^2\bar{\bar{c}}(s, p, z)}{dz^2} - (p^2 + s)\bar{\bar{c}}(s, p, z) = 0$$

where p is now a Fourier variable. Solving this equation and applying an inverse Laplace transformation, as was done above, again leads to eqn. (17). Inverse Fourier transformation [48] applied to that equation yields

$$c(t, x) = -\frac{1}{2\pi}\int_{-\infty}^{\infty} du \int_0^t \frac{\exp\left[-(x-u)^2/4(t-\tau)\right]}{t-\tau} f(\tau, u)\, d\tau \tag{56}$$

Combining eqns. (56) and (54) and taking into account that beyond the conductive surface $f(t, x) = 0$, one can write

$$\frac{f(t, x)\, \exp(\alpha fn[E(t) - E^\circ])/\Lambda + 1}{1 + \exp\{fn[E(t) - E^\circ]\}}$$

$$= -\frac{1}{2\pi}\int_A du \int_0^t \frac{\exp\left[-(x-u)^2/4(t-\tau)\right]}{t-\tau} f(\tau, u)\, d\tau \tag{57}$$

Equation (57) is much simpler than eqn. (24) proposed for a disk. It does not contain any special functions; therefore the computations should be much faster. Indeed, eqn. (24) has a singularity of type $(t-\tau)^{-3/2}$ which is not very easy to handle. The singularity of eqn. (57) is simpler.

Our results differ from those obtained by Coen et al. [25] in two ways. These authors used a boundary condition $0 < t,\ x \in A,\ z = 0;\ c(t, x) = 0$ instead of a general Butler–Volmer equation. As a result, only a chronoamperogram under diffusion control can be computed from their equation. They also chose not to use inverse Laplace transformation and had to deal with numerical inversion in addition to solving a quite complicated integral equation. The computations with eqn. (57) should be much easier.

Since the Fourier transformation used in this section, analogous to Hanckel transformation, requires only piecewise continuity of the diffusional flux as a function of x, we do not need to assume continuity of the conductive surface A. Instead, the solution (eqn. (57)) can be used to describe not only a single microband electrode (the limits of integration in eqn. (57) for this case are from -1 to 1), but also an array of the parallel microbands separated by the insulating gaps [49].

A set of arbitrarily-shaped planar electrodes embedded in an insulating plane

This general case encompasses several well-known electrochemical systems, e.g. an array of microelectrodes (Fig. 3), an electrode with a partially blocked surface,

islands of a growing film, etc. The three-dimensional diffusion problem is similar to that solved in a previous section:

$$\frac{\partial C_{Ox}}{\partial T} = D\left(\frac{\partial^2 C_{Ox}}{\partial X^2} + \frac{\partial^2 C_{Ox}}{\partial Y^2} + \frac{\partial^2 C_{Ox}}{\partial Z^2}\right)$$

$$0 < T,\ -\infty < X < \infty,\ -\infty < Y < \infty,\ 0 < Z \tag{58}$$

$$\frac{\partial C_R}{\partial T} = D\left(\frac{\partial^2 C_R}{\partial X^2} + \frac{\partial^2 C_R}{\partial Y^2} + \frac{\partial^2 C_R}{\partial Z^2}\right)$$

$$T = 0,\ -\infty < X < \infty,\ -\infty < Y < \infty,\ 0 < Z \qquad C_{Ox}(T, X, Y, Z) = C^\circ_{Ox}$$

$$C_R(T, X, Y, Z) = 0 \tag{59}$$

$$0 < T,\ X^2 + Y^2 + Z \to \infty \qquad C_{Ox}(T, X, Y, Z) \to C^\circ_{Ox} \qquad C_R(T, X, Y, Z) \to 0 \tag{60}$$

$$0 < T,\ -\infty < X < \infty,\ -\infty < Y < \infty,\ Z = 0$$

$$f_{Ox}(T, X, Y) = D\left(\frac{\partial C_{Ox}}{\partial Z}\right)_{Z=0} = -D\left(\frac{\partial C_R}{\partial Z}\right)_{Z=0} = \frac{i(T, X, Y)}{nF} \tag{61}$$

With new variables

$$t = DT,\ c = 1 - \frac{C_{Ox}}{C^\circ_{Ox}}$$

$$f(t, X, Y) = \left[\frac{\partial C(t, X, Y, Z)}{\partial Z}\right]_{z=0} = -\frac{1}{C^\circ_{Ox} D} f_{Ox}(T, X, Y) \tag{62}$$

we have

$$\frac{\partial c}{\partial t} = D\left(\frac{\partial^2 c}{\partial X^2} + \frac{\partial^2 c}{\partial Y^2} + \frac{\partial^2 C_{Ox}}{\partial Z^2}\right) \qquad 0 < t,\ -\infty < X < \infty,\ -\infty < Y < \infty,\ 0 < Z \tag{63}$$

$$t = 0,\ -\infty < X < \infty,\ -\infty < Y < \infty,\ 0 < Z \qquad c(t, X, Y, Z) = 0 \tag{64}$$

$$0 < t,\ X^2 + Y^2 + Z \to \infty \qquad c(t, X, Y, Z) \to 0 \tag{65}$$

$$0 < t,\ (X, Y) \in A,\ z = 0 \qquad f(t, X, Y) = \frac{\left(1 + \exp\{fn[E(t) - E^\circ]\}\right)c(t, x) - 1}{\exp\{\alpha fn[E(t) - E^\circ]\} D/k_s}$$

$$(X, Y) \notin A,\ f(t, X, Y) = 0 \tag{66}$$

Applying to this problem a double Fourier transformation with respect to X and Y, and a Laplace transformation with respect to t, yields

$$\frac{d^2 \bar{\bar{c}}(s, p, u, z)}{dz^2} - (p^2 + u^2 + s)\bar{\bar{c}}(s, p, u, z) = 0, \tag{67}$$

where p and u are the two Fourier variables. Solution of eqn. (67) is completely analogous to that of eqn. (15) and leads to

$$\bar{\bar{c}}(s, p, u) = -\frac{\bar{\bar{f}}(s, p, u)}{(p^2 + u^2 + s)^{1/2}} \tag{68}$$

After applying inverse Fourier and Laplace transformations, we have

$$c(t, X, Y) = -\frac{1}{4\pi^{3/2}} \int_{-\infty}^{\infty} \int_{-\infty}^{\infty} \int_{0}^{t} \frac{\exp\left\{-\left[(x-v)^2 + (y-w)^2\right]/4(t-\tau)\right\}}{(t-\tau)^{3/2}} \times f(\tau, v, w)\, d\tau\, dv\, dw \tag{69}$$

Substituting the boundary condition (66) into eqn. (69) results in

$$\frac{f(t, X, Y)\, \exp\{\alpha fn[E(t) - E^\circ]\} D/k_s + 1}{1 + \exp\{fn[E(t) - E^\circ]\}} = -\frac{1}{4\pi^{3/2}} \int_{A} \int\int_{0}^{t} \frac{\exp\left\{-\left[(x-v)^2 + (y-w)^2\right]/4(t-\tau)\right\}}{(t-\tau)^{3/2}} \times f(\tau, v, w)\, d\tau\, dv\, dw \tag{70}$$

We cannot compare eqn. (70) with any results reported previously; no analytical or numerical solution has been reported for this general problem. The numerical solution of this integral equation should be more complicated than those discussed above. We show below that it would lead to significant advantages compared with other known approaches.

Electrodes surrounded by an insulator of finite width

The finite size of the insulating sheath enclosing a microelectrode results in additional complexity. Shoup and Szabo [50] suggested an approximate numerical solution for a microdisk. To our knowledge, no analytical approaches to solving this problem have been reported. At the same time, neglecting the diffusional flux from the back side of the electrode may lead to errors [50]. For example, this contribution may be substantial in SECM, especially with an insulating substrate. We consider here only the case of a microdisk; however, the simple analysis shows the applicability of this approach in describing other planar electrodes, e.g. a microband or an SECM tip.

The plane containing the electrode surface divides the whole space into two half-spaces: the first one (the "front half-space" (Fig. 4(a)) is the usual diffusion space of the inlaid electrode; the second one (the "back half-space" (Fig. 4(b)) is a source of additional diffusional flux connected with the finite radius of an insulator. We can consider the plane $z = 0$ as an imaginary border between these half-spaces. We can now formulate the boundary problem for a microdisk exactly as above:

$$\frac{\partial c}{\partial t} = \frac{\partial^2 c}{\partial z^2} + \frac{\partial^2 c}{\partial r^2} + \frac{1}{r}\frac{\partial c}{\partial r} \qquad 0 < t,\ 0 \le r,\ 0 < z \tag{71}$$

$$t = 0,\ r \ge 0,\ z > 0 \qquad c(t, r, z) = 0 \tag{72}$$

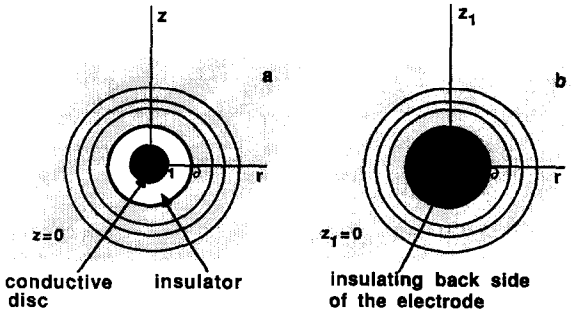

Fig. 4. A microdisk electrode embedded in an insulating ring. The "front half-space" (a) and the "back half-space" (b) are separated by the plane $z = 0$. For simplicity the thickness of a conductor connected with an electrode from the back side and the thickness of the disk are neglected. Thin circles represent the lines of the uniform concentration of electroactive species corresponding to cylindrical symmetry. From the back side the whole area of the disk and the surrounding insulator look like a homogeneous insulator. The plane $z_1 = 0$ (b) is identical with the plane $z = 0$ (a).

$$t > 0,\ r + z \to \infty \qquad c(t, r, z) \to 0 \tag{73}$$

$$t > 0,\ 0 \le r < 1,\ z = 0 \qquad f(t, r) = \frac{(1 + \exp\{fn[E(t) - E^\circ]\})c(t, r) - 1}{\exp\{\alpha fn[E(t) - E^\circ]\}/\Lambda}$$

$$1 < r < \partial,\ f(t, r) = 0 \quad \partial < r,\ f(t, r) = -g(t, r) \tag{74}$$

The only difference between formulations (9)–(12) and (71)–(74) is contained in eqn. (74), where beyond the conductive surface the diffusional flux is equal not to zero, but to the flux from the "back half-space" $g(t, r)$. Solving problem (71)–(74) exactly as above, we obtain the same eqns. (23) and (24). However, in this case the integration should be performed over the whole r-axis, from 0 to ∞, and the values of $f(t, r)$ for $r > \partial$ are unknown.

Let us consider the diffusion problem for the "back half-space" which preserves cylindrical symmetry:

$$\frac{\partial c}{\partial t} = \frac{\partial^2 c}{\partial z_1^2} + \frac{\partial^2 c}{\partial r^2} + \frac{1}{r}\frac{\partial c}{\partial r} \qquad 0 < t,\ 0 \le r,\ 0 < z_1 \tag{75}$$

$$t = 0,\ r \ge 0,\ z_1 > 0 \qquad c(t, r, z_1) = 0 \tag{76}$$

$$t > 0,\ r + z_1 \to \infty \qquad c(t, r, z_1) \to 0 \tag{77}$$

$$t > 0,\ 0 \le r < \partial,\ z_1 = 0 \quad g(t, r) = 0 \qquad \partial < r,\ g(t, r) = -f(t, r) \tag{78}$$

Reproducing the sequence of steps (14)–(22), one arrives at an expression virtually identical with eqn. (23):

$$c(t, r) = -\frac{1}{2\sqrt{\pi}} \int_\rho^\infty u\, du \int_0^t \frac{\exp[-(r^2 + u^2)/4(t - \tau)]}{(t - \tau)^{3/2}} I_0\left[\frac{ru}{2(t - \tau)}\right] g(\tau, u)\, d\tau \tag{79}$$

For $r > \partial$, $c(t, r)$ in eqn. (79) is the same value as that in eqn. (23) because the planes $z = 0$ and $z_1 = 0$ are identical. Combining eqns. (23), (79) and (78), we have

$$\int_0^\infty u\,\mathrm{d}u \int_0^t \frac{\exp\left[-(r^2+u^2)/4(t-\tau)\right]}{(t-\tau)^{3/2}} I_0\left[\frac{ru}{2(t-\tau)}\right] f(\tau, u)\,\mathrm{d}\tau$$

$$= -\int_\rho^\infty u\,\mathrm{d}u \int_0^t \frac{\exp\left[-(r^2+u^2)/4(t-\tau)\right]}{(t-\tau)^{3/2}} I_0\left[\frac{ru}{2(t-\tau)}\right] f(\tau, u)\,\mathrm{d}\tau \qquad (80)$$

or

$$\int_0^\partial u\,\mathrm{d}u \int_0^t \frac{\exp\left[-(r^2+u^2)/4(t-\tau)\right]}{(t-\tau)^{3/2}} I_0\left[\frac{ru}{2(t-\tau)}\right] f(\tau, u)\,\mathrm{d}\tau$$

$$= -2\int_\partial^\infty u\,\mathrm{d}u \int_0^t \frac{\exp\left[-(r^2+u^2)/4(t-\tau)\right]}{(t-\tau)^{3/2}} I_0\left[\frac{ru}{2(t-\tau)}\right] f(\tau, u)\,\mathrm{d}\tau \qquad (81)$$

The combination of eqns. (24) and (81) represents a solution of the problem under consideration. We do not expect any significant additional computational efforts in solving this problem compared with the single eqn. (24).

RESULTS AND DISCUSSION

Numerical solution of multidimensional integral equations

We present here only some basic ideas about the numerical solution of eqn. (24). Since this problem is new, various algorithms can be proposed, and many practical details will be discussed in a separate paper. The numerical solution of eqn. (24) requires one to build a temporal grid for the function $f(t, r)$ and to choose the sequence of r-points within the interval (0, 1). The temporal grid should be non-uniform, because this kinetic equation is stiff, like those solved previously [30–33]. The authors of most studies (excluding ref. 24) suggest using a different size for the distance between points on a disk surface with smaller steps near the border. Our computations did not show a dramatic difference in the results obtained with a uniform and a non-uniform distribution of r-points. However, a non-uniform distribution appeared to be somewhat more efficient (assuming the same number of points). An example of an appropriate space grid is given in the next section.

The integral equation to be solved is of a "mixed" type; the inner integral looks like a convolution integral of the Volterra type and the outer integral is of the Fredholm type [39,40]. The method of solution we have chosen is usual for Volterra equations. For each new point t_k of the temporal grid the value of the double integral is calculated anew, and the value of $f(t_k)$ is found by solving an algebraic equation. However, unlike one-dimensional Volterra equations [2–4,30–33], we now have to solve not a single algebraic equation, but a system of m linear equations at each step of integration to find m values of $f(t_k, r_i)$ for all r-points.

There are two different approaches to digitizing eqn. (24): interpolating $f(t, r)$ [17–20,25,29] or using some simple quadrature rule (e.g. trapezoid or mid-point rules) [2–4,30–33]. Since two-dimensional interpolation is not very easy, we shall discuss here only the second approach. An obvious expression for the inner integral in eqn. (24) at the kth step of the integration process is

$$\int_0^{t_k} \frac{\exp\left[-(r^2+u^2)/4(t_k-\tau)\right]}{(t_k-\tau)^{3/2}} I_0\left(\frac{ru}{2(t_k-\tau)}\right) f(\tau, u)\, d\tau$$
$$= \int_0^{t_{k-1}} \frac{\exp\left[-(r^2+u^2)/4(t_k-\tau)\right]}{(t_k-\tau)^{3/2}} I_0\left[\frac{ru}{2(t_k-\tau)}\right] f(\tau, u)\, d\tau$$
$$+ \int_{t_{k-1}}^{t_k} \frac{\exp\left[-(r^2+u^2)/4(t_k-\tau)\right]}{(t_k-\tau)^{3/2}} I_0\left[\frac{ru}{2(t_k-\tau)}\right] f(\tau, u)\, d\tau \tag{82}$$

It should be noted that only the last term in eqn. (82) contains the unknown value $f(t_k, u)$ as well as a singularity at $\tau = t_k$. The trapezoid rule for the first integral in the right-hand part of eqn. (82) is

$$\int_0^{t_{k-1}} \frac{\exp\left[-(r^2+u^2)/4(t_k-t)\right]}{(t_k-t)^{3/2}} I_0\left(\frac{ru}{2(t_k-\tau)}\right) f(\tau, u)\, d\tau$$
$$= \sum_{i=1}^{k-1} \frac{\exp\left[-(r^2+u^2)/4(t_k-t_i)\right]}{(t_k-t_i)^{3/2}} I_0\left(\frac{ru}{2(t_k-t_i)}\right) f(t_i, u)\Delta t_i \tag{83}$$

where $\Delta t_i = (t_{i+1} - t_{i-1})/2$ for $1 < i < k-1$, $\Delta t_1 = t_2/2$ and $\Delta t_{k-1} = (t_{k-1} - t_{k-2})/2$.

We cannot use the trapezoid rule for the last integral in eqn. (82) because it contains a singularity. It should be expressed as

$$\int_{t_{k-1}}^{t_k} \frac{\exp\left[-(r^2+u^2)/4(t_k-\tau)\right]}{(t_k-\tau)^{3/2}} I_0\left[\frac{ru}{2(t_k-\tau)}\right] f(\tau, u)\, d\tau$$
$$= \frac{f(t_{k-1}, u) + f(t_k, u)}{2} \int_{t_{k-1}}^{t_k} \frac{\exp\left[-(r^2+u^2)/4(t_k-\tau)\right]}{(t_k-\tau)^{3/2}} I_0\left[\frac{ru}{2(t_k-\tau)}\right] d\tau \tag{84}$$

Combining eqns. (82)–(84), we have

$$\int_0^{t_k} \frac{\exp\left[-(r^2+u^2)/4(t_k-\tau)\right]}{(t_k-\tau)^{3/2}} I_0\left[\frac{ru}{2(t_k-\tau)}\right] f(\tau, u)\, d\tau$$
$$= \sum_{i=1}^{k-1} \frac{\exp\left[-(r^2+u^2)/4(t_k-t_i)\right]}{(t_k-t_i)^{3/2}} I_0\left[\frac{ru}{2(t_k-t_i)}\right] f(t_i, u)\Delta t_i$$
$$+ \frac{f(t_{k-1}, u) + f(t_k, u)}{2} \int_{t_{k-1}}^{t_k} \frac{\exp\left[-(r^2+u^2)/4(t_k-\tau)\right]}{(t_k-\tau)^{3/2}} I_0\left[\frac{ru}{2(t_k-\tau)}\right] d\tau \tag{85a}$$

$$= F(r, u, t_{k-1}) + \frac{f(t_k, u)}{2} \int_{t_{k-1}}^{t_k} \frac{\exp\left[-(r^2+u^2)/4(t_k-\tau)\right]}{(t_k-\tau)^{3/2}} I_0\left[\frac{ru}{2(t_k-\tau)}\right] d\tau \tag{85b}$$

where $F(r, u, t_{k-1})$ involves terms in t_{k-1} in eqn. (85a), i.e. a combination of terms on the right-hand side of eqn. (85a).

Now one can use eqn. (85) to obtain an expression for the double integral. For the outer integral we suggest use of a slightly modified mid-point rule instead of the trapezoid rule because our computations have shown a very poor performance of the last quadrature with a non-uniform spatial grid, which seems to be connected with some symmetry problems. The following quadrature showed much better results:

$$\int_0^1 u\, du \int_0^{t_k} \frac{\exp\left[-(r^2+u^2)/4(t-\tau)\right]}{(t_k-\tau)^{3/2}} I_0\left[\frac{ru}{2(t_k-\tau)}\right] f(\tau, u)\, d\tau$$

$$= \int_0^1 u \left\{ F(r, u, t_{k-1}) + \frac{f(t_k, u)}{2} \int_{t_{k-1}}^{t_k} \frac{\exp\left[-(r^2+u^2)/4(t_k-\tau)\right]}{(t_k-\tau)^{3/2}} \right.$$

$$\left. \times I_0\left[\frac{ru}{2(t_k-\tau)}\right] d\tau \right\} du$$

$$= \sum_{j=1}^{m} u_j F(r, u_j, t_{k-1}) \Delta u_j + \int_0^1 \frac{f(t_k, u)}{2} u\, du \int_{t_{k-1}}^{t_k} \frac{\exp\left[-(r^2+u^2)/4(t_k-\tau)\right]}{(t_k-\tau)^{3/2}}$$

$$\times I_0\left[\frac{ru}{2(t_k-\tau)}\right] d\tau$$

$$= \sum_{j=1}^{m} \left\{ u_j F(r, u_j, t_{k-1}) \Delta u_j + \frac{f(t_k, u_j)}{2} \int_{a_{j-1}}^{a_j} u\, du \int_{t_{k-1}}^{t_k} u \right.$$

$$\left. \times \frac{\exp\left[-(r^2+u^2)/4(t_k-\tau)\right]}{(t_k-\tau)^{3/2}} I_0\left(\frac{ru}{2(t_k-\tau)}\right) d\tau \right\} \tag{86}$$

where each point u_j (excluding two points u_1 and u_m) is located in the middle of

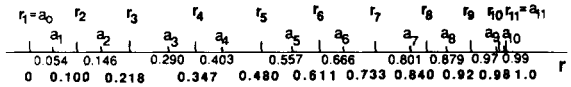

Fig. 5. Non-uniform spatial grid over the disk surface. Bold type and high bars correspond to the points r_i in which the local flux is to be computed. Light face type and low bars indicate the boundaries a_i of integration subintervals. It should be noted that $r_i - a_i = a_{i+1} - r_i$ for all points excluding the first and the last.

the interval (a_{j-1}, a_j) (Fig. 5) and $\Delta u_j = a_j - a_{j-1}$. Substitution of eqn. (86) into eqn. (24) leads to a system of m linear equations for a given time t_k:

$$d(t_k)f(t_k, r_1) + \frac{1}{2}\sum_{j=1}^{m} f(t_k, r_j)\int_{a_{j-1}}^{a_j} u\,\mathrm{d}u \int_{t_{k-1}}^{t_k} u \frac{\exp\left[-(r_1^2+u^2)/4(t_k-\tau)\right]}{(t_k-\tau)^{3/2}} \times I_0\left[\frac{r_1 u}{2(t_k-\tau)}\right] \mathrm{d}\tau = \mathrm{RH}(t_k) - \sum_{j=1}^{m} u_j F(r_1, u_j, t_{k-1})\Delta u_j$$

$$\vdots \qquad (87)$$

$$d(t_k)f(t_k, r_m) + \frac{1}{2}\sum_{j=1}^{m} f(t_k, r_j)\int_{a_{j-1}}^{a_j} u\,\mathrm{d}u \int_{t_{k-1}}^{t_k} u \frac{\exp\left[-(r_m^2+u^2)/4(t_k-\tau)\right]}{(t_k-\tau)^{3/2}} \times I_0\left[\frac{r_m u}{2(t_k-\tau)}\right] \mathrm{d}\tau = \mathrm{RH}(t_k) - \sum_{j=1}^{m} u_j F(r_m, u_j, t_{k-1})\Delta u_j$$

where

$$d(t_k) = \frac{2\sqrt{\pi}\,\exp\{\alpha fn[E(t_k) - E^\circ]\}}{\Lambda(1 + \exp\{fn[E(t_k) - E^\circ]\})}$$

$$\mathrm{RH}(t_k) = -\frac{2\sqrt{\pi}}{1 + \exp\{fn[E(t_k) - E^\circ]\}}$$

This system can be written in matrix form as

$$\mathbf{A}\boldsymbol{f} = \boldsymbol{b} \qquad (88)$$

where the components of the vectors $\boldsymbol{f}$ and $\boldsymbol{b}$ are $f_j = f(t_k, r_j)$ and

$$b_i = \mathrm{RH}(t_k) - \sum_{j=1}^{m} u_j F(r_i, u_j, t_{k-1})\Delta u_j$$

The elements of the matrix **A** are

$$a_{ij}|_{i \neq j} = \frac{1}{2}\int_{a_{j-1}}^{a_j} u\,\mathrm{d}u \int_{t_{k-1}}^{t_k} u \frac{\exp\left[-(r_i^2+u^2)/4(t_k-\tau)\right]}{(t_k-\tau)^{3/2}} I_0\left[\frac{r_i u}{2(t_k-\tau)}\right] \mathrm{d}\tau$$

and

$$a_{ii} = d(t_k) + \frac{1}{2}\int_{a_{j-1}}^{a_j} u\,\mathrm{d}u \int_{t_{k-1}}^{t_k} u \frac{\exp\left[-(r_i^2+u^2)/4(t_k-\tau)\right]}{(t_k-\tau)^{3/2}} I_0\left(\frac{r_i u}{2(t_k-\tau)}\right) \mathrm{d}\tau$$

Solving system (88) one can obtain m values of the flux $f(t_k, r_j)$ and compute the total current according to eqn. (13).

The most serious problem in solving eqn. (24) is handling the integrand singularity. There are two different cases: $i \neq j$ and $i = j$. In the first case the singularity is removable; if the point r_i does not belong to the interval (a_{j-1}, a_j), for any $u \in (a_{j-1}, a_j)$,

$$\lim_{\tau \to t_k} u \frac{\exp\left[-\left(r_i^2 + u^2\right)/4(t_k - \tau)\right]}{(t_k - \tau)^{3/2}} I_0\left(\frac{r_i u}{2(t_k - \tau)}\right) = 0.$$

Therefore the one-dimensional integral (85) is convergent, and the matrix elements can be computed:

$$a_{ij}|_{i \neq j} = \frac{r_j(a_j - a_{j-1})}{2} \int_{t_{k-1}}^{t_k} \frac{\exp\left[-\left(r_i^2 + r_j^2\right)/4(t_k - \tau)\right]}{(t_k - \tau)^{3/2}} I_0\left(\frac{r_i r_j}{2(t_k - \tau)}\right) d\tau \qquad (89)$$

If $i = j$, the integrand at the point $u = r_i$ is

$$r_i \frac{\exp\left[-r_i^2/2(t_k - \tau)\right]}{(t_k - \tau)^{3/2}} I_0\left(\frac{r_i^2}{2(t_k - \tau)}\right)$$

Since $\exp(-x) I_0(x) \approx x^{-1/2}$ for $x \to \infty$ [51], the integrand has a singularity of the type $(t_k - \tau)^{-1}$ for $\tau \to t_k$, and the integral (85) does not converge. However, an analysis has shown that the double integral (86) still exists and can be computed directly using an adaptive quadrature. Computing double integrals for m values of r_i and for each time is the longest part of the computations. Since the values of integrals are independent of kinetic parameters and of $E(t)$, we suggest that they are computed once (when temporal and spatial grids are established) and then stored in a special file for further use.

The computations have shown a surprising peculiarity of multidimensional integral equations—the best stability and accuracy of the solution is achieved by choosing an extremely small initial time step and a very large coefficient of temporal grid expansion. For example, the transients shown in Fig. 6 were computed with the following temporal grid:

$$t_1 = 0,\ h_1 \approx 10^{-23} \quad \text{for } i = 1, \ldots \quad t_{i+1} = t_i + h_i \quad h_{i+1} = h_i \times \mathrm{TEXP}_i \qquad (90)$$

where $\mathrm{TEXP}_i = \mathrm{TEXP}_{i-1} - 0.7 + 0.0175(i - 2)$ is a changeable expansion coefficient, and $\mathrm{TEXP}_1 = 15.093$. The transients computed using this temporal grid have only 17 t-points over the dimensionless time interval $(10^{-4}, 100)$. Notice that 17 points is enough to compute a quite accurate transient for the whole time range. Certainly, a user can choose a less rapidly expanding grid. For example, the cyclic voltammograms (CVs) discussed below were computed using a smaller $\mathrm{TEXP}_1 = 3.95$. A rapidly expanding temporal grid is probably suitable for any type of stiff kinetic equation. We used it for solving the one-dimensional Volterra equations reported previously [30–33] and obtained very accurate solutions and a significant gain in CPU time.

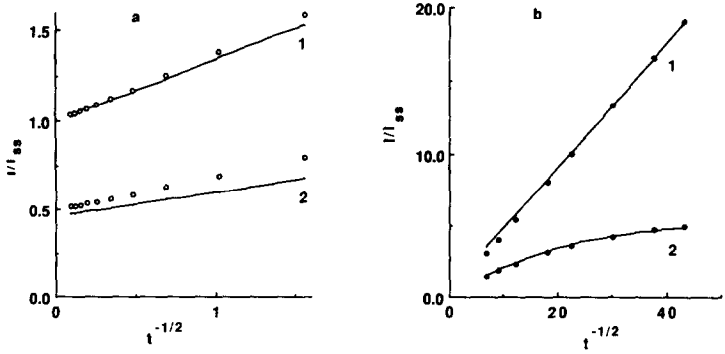

Fig. 6. Dimensionless quasi-reversible transients at a microdisk electrode computed from eqn. (24) with $\Lambda = 10$, $n = 1$ and $\alpha = 0.5$: curves 1, $E = -0.2$ V; curves 2, $E = 0$ V. (a) Long-time region; open circles are calculated from the Shoup–Szabo equation [13]. (b) Short-time region; closed circles are computed from the quasi-reversible chronoamperogram equation [52].

Comments on programming and computations

FORTRAN-77 programs implementing the given algorithm include four standard subroutines from the IMSL Program Library [53,54]: subroutine LSARG solves the linear system (88); QDAG and TWODQ evaluate the values of integrals (85) and double integrals (86) respectively using a globally adaptive scheme based on Gauss–Kronrod rules; BSI0E computes the exponentially scaled Bessel function $\exp(-x)I_0(x)$.

The programs were executed on a CRAY Y-MP/864 supercomputer. This was used because of (i) the absence of any preliminary information about the algorithm resource requirements, (ii) the availability of numerous program libraries and (iii) our intention to solve more complicated problems in the future (see the Theory section). Actually, computation of any transient presented below required less than 3 s of CPU time (using an established r- and t-grid). Since this algorithm performs numerous evaluations of special functions, it is not vectorizable. In this case, the CRAY was only about two orders faster than a PC-level computer. Thus these computations should require only a few minutes of microcomputer CPU time.

Potentiostatic transients at a microdisk

We could not find any published results for chronoamperograms at a disk electrode under mixed diffusion–kinetic control. These curves are much harder to compute than the well-known diffusion-controlled transients with constant surface concentration [9–14,17–20,23,24], because of the stiffness of the kinetic equations. Therefore, we compared our quasi-reversible chronoamperograms (Fig. 6) with those calculated using the Shoup–Szabo equation [13], which has been claimed to be accurate to 0.6%. As expected, both curves at high negative potentials (curves 1) are coincident over the long-time region. Deviations should be observed at short times when the process is kinetically controlled. At $E = E^\circ$, a quasi-reversible

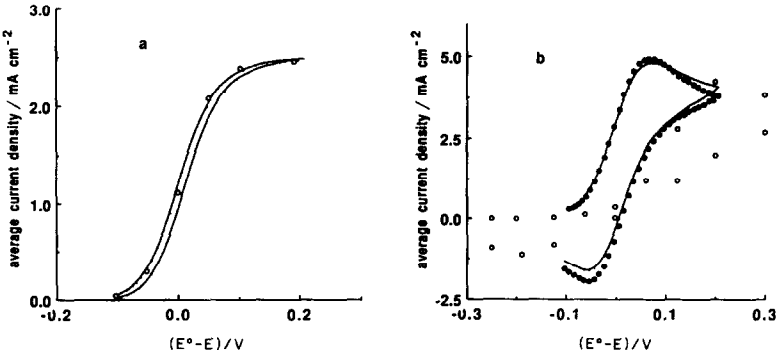

Fig. 7. Quasi-reversible CVs at a microdisk electrode computed from eqn. (24): $\Lambda = 5$, $n = 1$, $\alpha = 0.5$. (a) Near-steady-state CV, $v = 10$ mV s^{-1}; open circles are obtained from ref. 23. (b) Non-steady-state CVs, $v = 20$ V s^{-1}; open circles are obtained from [23], and closed circles are computed for a hemispherical electrode with the same radius (5 μm) and the same values of parameters using the techniques of refs. 30–33.

steady-state current is somewhat lower than the reversible current (curves 2) in agreement with ref. 12.

There is another approach to checking the short-time part of the kinetic transient. When $I(t) \gg I_{ss}$, the influence of the edge effect is negligible and the current corresponds to the well-known equations derived for planar diffusion. Therefore the transient (non-steady-state) behavior of this electrode can be described exactly using the equation of a quasi-reversible chronoamperogram [52]. The transients calculated from that equation and converted to dimensionless form are in good agreement with our data (Fig. 6(b)). At longer times, the influence of the steady-state current becomes substantial and deviations arise.

Cyclic voltammograms

There is quite a good coincidence between the steady-state CVs at a microdisk electrode computed by different authors. Our quasi-reversible CV approaching steady-state behavior (Fig. 7(a)) is in agreement with the results of Taylor et al. [23] which have been verified by comparison with the analytical approximation of ref. 12. At the same time, no reliable data have been computed so far for quasi-reversible non-steady-state CVs. References 15, 16, 23 and 55 do not contain quantitative comparisons with the results of other authors. Michael et al. [55] claimed only qualitative agreement of their simulated CV with that of Heinze and Storzbach [16]. A simple analysis shows rather large differences between the curves given in ref. 23 and and those in refs. 15, 16 and 55. A comparison of our quasi-reversible non-steady-state CV (Fig. 7(b)) with that of Taylor et al. [23] shows substantial discrepancies, the most important or which is in values of peak potentials. Thus, for $\alpha = 0.5$, $\Lambda = 5$, and $v = 20$ V s^{-1}, our results show $\Delta E_p = 130$ mV compared with $\Delta E_p \approx 400$ mV in ref. 23. We can analyze these differences. First, since this is

a non-steady-state voltammogram, it should be similar to that for a large planar electrode. The ΔE_p value for the same kinetic parameters in ref. 56 is about 100 mV. Second, we computed the CV at a hemispherical electrode (which should be much like a microdisk CV) with the same kinetic parameters (Fig. 7(b)) using the technique of refs. 30–33; $\Delta E_p = 135$ mV was found. From ref. 15 one can obtain for the same case $\Delta E_p \approx 135$ mV. ΔE_p in the range 100–200 mV is obtained from the equations in refs. 16 and 55. All these values are compatible with our calculations, but not with those based on ref. 23.

Integral equations versus numerical simulations

Digital simulations based on finite difference and finite element methods have been widely used in the modeling of electrochemical systems because they can be readily applied without a mathematically sophisticated background and allow straightforward and minor modifications to incorporate chemical reactions coupled to the heterogeneous electron transfer reaction. They become less efficient and more difficult to apply to problems involving multidimensional electrode geometries, such as those considered here, or to those involving very different spatial scales, e.g. when the coupling of double-layer charging or semiconductor space charge effects to diffusion in solution is treated.

An important advantage of the technique described here is a drastic reduction of the requirement in computer resources. For instance, numerical simulation of a microdisk requires at least $100 \times 100 = 10^4$ (r, z) points [23,24]. With 1000 time iterations as used in ref. 23 for either transient or CV simulation, the time–space grid has as many as 10^7 nodes. In contrast, reducing the problem to the integral equation leads to the decrease of its dimension by one. Additionally, in solving integral equations one can use only a few r-points over the electrode surface without losing accuracy. For instance, in refs. 19 and 20 the use of no more than 10 r-points over the disk surface was recommended. Analogously, we have found that a space grid with 11 r-points (Fig. 5) is quite enough to compute accurate polarization curves for a microdisk. Moreover, no r-nodes are necessary beyond the conductive surface. This circumstance is particularly important in the case of electrode arrays, partially blocked electrodes, and other electrochemical systems in which the active electrodes are widely spaced by insulating areas. These would require large amounts of computation time using any type of digital simulation, because the whole surface must be covered with a spatial grid, and an expanding grid is difficult to devise for the general case (see Theory section).

As discussed above, the integral equation approach allows the use of a rapidly expanding initial part of the temporal grid and only a few spatial points; consequently, there are only about 1000 elements in our largest array of $f(t, r)$. Although at this stage we were more concerned with the accuracy and stability of our program than in optimization, it appeared to be about two orders faster than an efficient Krylov integrator [57,58]. Finally, the technique described seems to be a good method for modeling electrochemical systems which involve complex

geometry, while digital simulation is the only feasible way to treat processes with coupled chemical stages of higher orders.

CONCLUSIONS

Multidimensional integral equations are suitable for modeling complicated electrochemical systems. Although no standard software is presently available for solving the types of equations, simple and efficient algorithms can be created. Solving the integral equations was about as efficient as numerical simulations for one-dimensional problems [30–33]. It was significantly more efficient for relatively simple two-dimensional systems like a microdisk and should be much better for modeling more complicated objects. Many physical problems relying on partial differential equations can be transformed to multidimensional integral equations. Numerical solution of such equations can be used, for example, in heat transfer calculations (which are very much like diffusion problems) as well as in other physical applications.

ACKNOWLEDGEMENTS

The support of this research by SACHEM and the National Science Foundation (CHE 8901450) is gratefully acknowledged. Our thanks are due to Dr. G. Denuault for helpful discussions. The computing resources for this work were provided by The University of Texas System Center for High Performance Computing.

Nomenclature

A	electrode surface area (conductive surface)
$C(T, X, Y, Z)$, $C(T, R, Z)$	concentrations of the electroactive species as functions of spatial variables and time; the subscripts Ox and R relate to the oxidized and reduced forms respectively
$c(t, x, y, z)$, $c(t, r, z)$	the same variables in dimensionless form
$C(T, R)$	surface concentrations of the electroactive species
$c(t, r)$	the same variables in dimensionless form
C°	bulk concentration
D	diffusion coefficient
$E(T)$, $E(t)$	instantaneous value of the electrode potential
E°	standard (formal) potential
$f(T, X, Y)$, $f(T, R)$	diffusion flux towards the electrode surface
$f(t, r)$	the same variables in dimensionless form
f	$= F/RT$
$I(T)$, $I(t)$	faradaic current and the same variable in dimensionless form
I_{ss}	$4nFC^\circ DR_0$, microdisk steady-state current

$i(T, R)$, $i(T, X, Y)$	local faradaic current density
k_s	standard rate constant for heterogeneous ET reaction
w	microband width
L	distance between tip and substrate electrodes in SECM
n	number of electrons involved in electrode reaction
R_0	radius of a disk electrode
R_1, R_2	tip and substrate radii respectively
υ	scan rate
α	transfer coefficient
∂	ratio of the radius of the insulating ring surrounding a microdisk to the disk radius
Λ, Λ_1, Λ_2	dimensionless kinetic parameters given by $wk_s/2D$, $R_0k_s^1/D$ and $R_0k_s^2/D$ respectively; subscript 1 relates to the tip and subscript 2 to the substrate electrode
γ	$=L/R_1$, dimensionless distance between two electrodes in SECM
δ	ratio of the substrate radius to the tip radius

REFERENCES

1 P. Delahay, New Instrumental Methods in Electrochemistry, Interscience, New York, 1954.
2 R.S. Nicholson and I. Shain, Anal. Chem., 36 (1964) 706.
3 R.S. Nicholson and I. Shain, Anal. Chem., 37 (1965) 178.
4 R.S. Nicholson and I. Shain, Anal. Chem., 37 (1965) 667.
5 W.H. Reinmuth, Anal. Chem., 33 (1961) 1793.
6 S.W. Feldberg, in A.J. Bard (Ed.), Electroanalytical Chemistry, Vol. 3, Marcel Dekker, New York, 1969, p. 199.
7 S. Pons, in A.J. Bard (Ed.), Electroanalytical Chemistry, Vol. 13, Marcel Dekker, New York, 1984, p. 115.
8 R.M. Wightman and D.O. Wipf, in A.J. Bard (Ed.), Electroanalytical Chemistry, Vol. 15, Marcel Dekker, New York, 1989, p. 267.
9 K. Aoki and J. Osteryoung, J. Electroanal. Chem., 122 (1981) 19.
10 K. Aoki and J. Osteryoung, J. Electroanal. Chem., 160 (1984) 335.
11 K.B. Oldham, J. Electroanal. Chem., 122 (1981) 1.
12 A.M. Bond, K.B. Oldham and C.G. Zoski, J. Electroanal. Chem., 245 (1988) 71.
13 D. Shoup and A. Szabo, J. Electroanal. Chem., 140 (1982) 237.
14 D. Shoup and A. Szabo, J. Electroanal. Chem., 160 (1984) 1.
15 J. Heinze, Ber. Bunsenges. Phys. Chem., 85 (1981) 1096.
16 J. Heinze and M. Storzbach, Ber. Bunsenges. Phys. Chem., 90 (1986) 1043.
17 M. Fleischmann and S. Pons, J. Electroanal. Chem., 250 (1988) 257.
18 M. Fleischmann, J. Daschbach and S. Pons, J. Electroanal. Chem., 263 (1989) 189.
19 M. Fleischmann, D. Pletcher, G. Denuault, J. Daschbach and S. Pons, J. Electroanal. Chem., 263 (1989) 225.
20 G. Denuault, Ph.D. Thesis, University of Southampton, 1989.
21 D.R. Baker and M.W. Verbrugge, J. Electrochem. Soc., 137 (1990) 1832.
22 D.R. Baker and M.W. Verbrugge, J. Electrochem. Soc., 137 (1990) 3836.

23 G. Taylor, H. Girault and J. McAleer, J. Electroanal. Chem., 293 (1990) 19.
24 D.J. Gavaghan and J.S. Rollet, J. Electroanal. Chem., 295 (1990) 1.
25 S. Coen, D.K. Cope and D.E. Tallman, J. Electroanal. Chem., 215 (1986) 29.
26 M.R. Deaken, R.M. Wightman and C.A. Amatore, J. Electroanal. Chem., 215 (1986) 49.
27 K. Aoki, K. Tokuda and H. Matsuda, J. Electroanal. Chem., 225 (1987) 19.
28 M. Fleischmann, S. Bandyopadhyay and S. Pons, J. Phys. Chem., 89 (1985) 5537.
29 D.K. Cope, C.H. Scott and D.E. Tallman, J. Electroanal. Chem., 285 (1990) 49.
30 M.V. Mirkin, A.P. Nilov and M.K. Nauryzbaev, J. Electroanal. Chem., 281 (1990) 41.
31 M.V. Mirkin and A.P. Nilov, J. Electroanal. Chem., 283 (1990) 35.
32 M.V. Mirkin and A.P. Nilov, Comput. Chem., 15 (1991) 55.
33 M.V. Mirkin, Comput. Chem., 15 (1991) 169.
34 A.J. Bard and L.R. Faulkner, Electrochemical Methods, Wiley, New York, 1980.
35 G.A. Korn and T.M. Korn, Mathematical Handbook for Scientists and Engineers, McGraw-Hill, New York, 1961, p. 230.
36 M. Abramowitz and I. Stegun (Eds.), Handbook of Mathematical Functions, Dover, New York, 1965, p. 358.
37 G.N. Watson, A. Treatise on the Theory of Bessel Functions, Cambridge University Press, Cambridge, 1962, p. 395.
38 M. Abramowitz and I. Stegun (Eds.), Handbook of Mathematical Functions, Dover, New York, 1965, p. 374.
39 R. Kress, Linear Integral Equations, Springer-Verlag, Berlin, 1989.
40 L.M. Delves, Computational Methods for Integral Equations, Cambridge University Press, Cambridge, 1986.
41 M.A. Golberg (Ed.), Numerical Solution of Integral Equations, Plenum Press, New York, 1990.
42 P.P. Zabreyko, A.I. Koselev, M.A. Krasnosel'skii, S.G. Mihlin, L.S. Rakovscik and V.Ya. Stacenko, Integral Equations—A Reference Text, Noordhoff, Leyden, 1975.
43 I.G. Graham, J. Aust. Math. Soc., Ser. B, 22 (1981) 456; Numerical Methods for Multidimensional Integral Equations, Tech. Rep. 12-1983, University of Melbourne, 1983.
44 A.J. Bard, F.-R.F. Fan, J. Kwak and O. Lev, Anal. Chem., 61 (1989) 132.
45 J. Kwak and A.J. Bard, Anal. Chem., 61 (1989) 1221.
46 H. Bateman, Tables of Integral Transforms, Vol. 1, McGraw-Hill, New York, 1954, p. 257.
47 H. Bateman, Tables of Integral Transforms, Vol. 1, McGraw-Hill, New York, 1954, p. 388.
48 F. Oberhettinger, Tabellen fur Fourier Transformation, Springer-Verlag, Berlin, 1957, p. 11.
49 A.J. Bard, J.A. Crayston, G.P. Kittlesen, T.V. Shea and M.S. Wrighton, Anal. Chem., 58 (1986) 2321.
50 D. Shoup and A. Szabo, J. Electroanal. Chem. Interfacial Electrochem., 160 (1984) 27.
51 M. Abramowitz and I. Stegun (Eds.), Handbook of Mathematical Functions, Dover, New York, 1965, p. 377.
52 P. Delahay, J. Am. Chem. Soc., 75 (1953) 1430.
53 IMSL MATH/LIBRARY. FORTRAN Subroutines for Mathematical Applications, Version 1.1, IMSL Inc., Houston, TX, 1989.
54 IMSL SFUN/LIBRARY. FORTRAN Subroutines for Evaluating Special Functions, Version 2.1, IMSL Inc., Houston, TX, 1989.
55 A.C. Michael, R.M. Wightman and C.A. Amatore, J. Electroanal. Chem., 267 (1989) 33.
56 R.S. Nicholson, Anal. Chem., 37 (1965) 1351.
57 A.J. Bard, G. Denuault, B.C. Dornblaser, R.A. Friesner and L.S. Tuckerman, Anal. Chem., 63 (1991) 1282.
58 G. Denuault, private communication 1990.